

## Effect of Nb Doping on the Dielectric and Strain Properties of Lead-free $0.94(\text{Bi}_{1/2}\text{Na}_{1/2})\text{TiO}_3\text{-}0.06\text{BaTiO}_3$ Ceramics

Hyung-Su Han, In-Ki Hong\*, Young-Min Kong\*, Jae-Shin Lee\*, and Wook Jo<sup>†</sup>

School of Materials Science and Engineering, Ulsan National Institute of Science and Technology, Ulsan 44919, Korea

\*School of Materials Science and Engineering, University of Ulsan, Ulsan 44610, Korea

(Received February 3, 2016; Revised March 18, 2016; Accepted March 21, 2016)

### ABSTRACT

$(\text{Bi}_{1/2}\text{Na}_{1/2})_{0.94}\text{Ba}_{0.06}(\text{Ti}_{1-x}\text{Nb}_x)\text{O}_3$  (BNBT $x$ Nb) ceramics were investigated in terms of the crystal structure as well as the ferroelectric, dielectric, and piezoelectric properties. While little change was observed in the microstructure except for a slight decrease in the average grain size, a significant change was noticed in the temperature dependence of dielectric and piezoelectric properties. It was shown that the property changes are closely related to the downward shift in the position of the ferroelectric-to-relaxor transition temperature with increasing amount of Nb doping. A special emphasis is put on the fact that Nb doping is so effective at decreasing the ferroelectric-to-relaxor transition temperature that even at no more than 2 at.% Nb addition, the transition temperature was already brought down slightly below room temperature, resulting in the birth of a large strain at 0.46 %, equivalent to  $S_{\text{max}}/E_{\text{max}} = 767$  pm/V.

**Key words :** Lead-free piezo ceramics, Relaxor ferroelectrics, Electromechanical strain

### 1. Introduction

Piezoelectric ceramics that interchangeably convert mechanical to electrical energy play key roles in micro-controllable sensors and actuators; in these ceramics, lead zirconate titanate (PZT) has been used as a primary material for more than five decades. However, over the past 20 years, environmental concerns about harmful elements have accelerated studies on lead-free piezoelectric ceramic alternatives to PZT that contains more than 60 wt% Pb.<sup>1-4</sup> Especially, Bi-based lead-free perovskite materials are one of the most promising candidates with respect to the replacement of PZT. The usual compositions in this category are bismuth sodium titanate ( $\text{Bi}_{1/2}\text{Na}_{1/2}\text{TiO}_3$ , BNT), bismuth potassium titanate ( $\text{Bi}_{1/2}\text{K}_{1/2}\text{TiO}_3$ , BKT), and solid solutions of these materials, such as BNT-BaTiO<sub>3</sub> (BNT-BT)<sup>5</sup> and BNT-BKT (BNKT) with a morphotropic phase boundary (MPB).<sup>6</sup>

Recently, incipient piezoelectricity as a new concept is considered to be one of the promising strategies to be used in large-stroke actuator applications because of the unusual strain properties of Bi-based materials.<sup>3</sup> In BNT-based or BNKT-based lead-free relaxor ceramics, the usual strain level reaches ~ 0.4 % with a small amount of chemical modifications,<sup>7-12</sup> which is almost twice the usual strain of PZT ceramics. This large electromechanical strain is

known to result from a reduction in the remanent strain,  $S_{\text{rem}}$ ,<sup>13</sup> due to the presence of a nonpolar phase (more precisely an ergodic relaxor, ER)<sup>14-16</sup> at 'zero' electric field. This means that this phenomenon is associated with a reversible electric-field-induced phase transformation from an ER phase to a ferroelectric (FE) phase.<sup>13,14</sup>

This study investigates the effect of Nb doping on the microstructure, the crystal structure, and the electrical properties of lead-free BNBT ceramics.

### 2. Experimental Procedure

Ceramic powders conforming to the chemical formula,  $(\text{Bi}_{1/2}\text{Na}_{1/2})_{0.94}\text{Ba}_{0.06}(\text{Ti}_{1-x}\text{Nb}_x)\text{O}_3$  (BNBT $x$ Nb,  $x = 0 \sim 6$  mol%), were synthesized using a conventional solid-state reaction route. Reagent grade  $\text{Bi}_2\text{O}_3$ ,  $\text{Na}_2\text{CO}_3$ ,  $\text{Nb}_2\text{O}_5$ , and  $\text{TiO}_2$  (99.9%, High Purity Chemicals, Japan) powders were used as raw materials. These raw materials were first put in a drying oven at 100 °C for 24 h to remove moisture and then weighed according to the stoichiometric formulas. The powders were ball-milled in ethanol with zirconia balls for 24 h, dried at 80 °C for 24 h, and calcined at 850 °C for 2 h in a covered alumina crucible. After calcination, the composite powder was mixed with polyvinyl alcohol (PVA) as a binder and then pressed into green discs with a diameter of 12 mm under a uniaxial pressure of 98 MPa. These green pellets were sintered at 1175 °C in a covered alumina crucible for 2 h in air.

The crystal structure was analyzed using an X-ray diffractometer (XRD, RAD III, Rigaku, Japan); the surface morphology was observed with a field-emission scanning

<sup>†</sup>Corresponding author : Wook Jo

E-mail : wookjo@unist.ac.kr

Tel : +82-52-217-2347 Fax : +82-52-217-2408

electron microscope (FE-SEM, JEOL, JSM-650FF, Japan); the average grain size was determined by linear intercept method.<sup>17</sup> For electrical measurements, a silver paste was screen printed on both sides of specimens and subsequently burnt in at 700 °C for 30 min. The polarization ( $P$ ) and strain ( $S$ ) hysteresis as a function of the external electric field ( $E$ ) were measured in silicon oil by using a modified Sawyer-Tower circuit and a linear variable differential transducer, respectively. The temperature-dependent dielectric constant ( $\epsilon_r$ ) and dielectric loss ( $\tan \delta$ ) of the BNBT $x$ Nb ceramics were recorded using an impedance analyzer (HP4192A) attached to a programmable furnace at the measurement frequencies of 1–100 kHz in a temperature range of 25–500 °C. The piezoelectric constant ( $d_{33}$ ) was determined using a Berlincourt  $d_{33}$ -meter after poling samples under a DC electric field of 5 kV/mm for 15 min in silicon oil.

### 3. Results and Discussion

Figures 1(a) and 1(b) provide SEM micrographs of a thermally etched surface, respectively, of BNBT0Nb and BNBT5Nb ceramics sintered at 1175 °C for 2 h; these images reveal dense microstructures regardless of the level of Nb doping. The relative density of all ceramics was measured and found to be over 98% of the theoretical density of each composition. It can be clearly seen that increasing the Nb concentration leads not only to a reduction in the average grain size but also to a narrower size distribution. The average

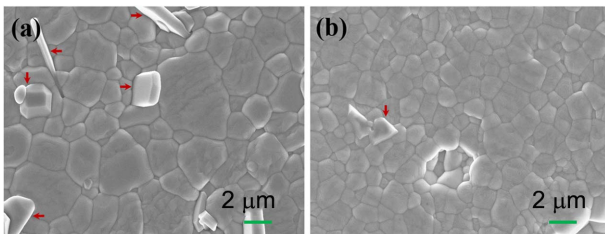


**Fig. 1.** FE-SEM micrographs of (a) BNBT0Nb ( $x = 0$ ) and (b) BNBT6Nb ( $x = 6$ ) (Red arrows correspond to a Birich foreign phase induced during thermal etching process).

grain size was found to decrease from about  $2.3 \pm 0.5 \mu\text{m}$  for BNBT0Nb to  $1.8 \pm 0.3 \mu\text{m}$  for BNBT6Nb ceramics.

X-ray diffraction patterns of the BNBT $x$ Nb ceramics in the  $2\theta$  range of  $20 \sim 80^\circ$  are shown in Fig. 2. All samples indicated a single perovskite structure without any secondary phase within the resolution limit of the adopted apparatus. BNBT0Nb ( $x = 0$ ) was analyzed to have a rhombohedral symmetry by the presence of a peak splitting around  $40^\circ$ . However, this rhombohedral symmetry tends to disappear with increasing Nb content, implied by the merge of split  $(111)_{\text{PC}}$  (the subscript 'pc' denotes 'pseudocubic') peak.

Figure 3 shows the temperature dependence of the dielectric permittivity ( $\epsilon_r$ ) and the corresponding dielectric loss ( $\tan \delta$ ) for poled (top) and unpoled (bottom) BNBT $x$ Nb ceramics in the frequency range of 1 to 100 kHz. On the unpoled samples, there are two distinctive dielectric anomalies. One is a strong frequency-dispersive region at lower temperature appearing as a shoulder (refer to the inset figure in (e)); the other is a relatively weak frequency-dispersive region in the higher temperature regime. These two anomalies can be explained as the consequences of the two successive dielectric relaxations of the low-temperature and high-temperature polar nanoregions (PNRs), bridged by an intermediate phase transformation between the two PNRs.<sup>14</sup> Although the origin of the high-temperature anomaly is still controversial, that of the low-temperature anomaly has been clearly shown to be due to the inherent relaxor nature of the system.

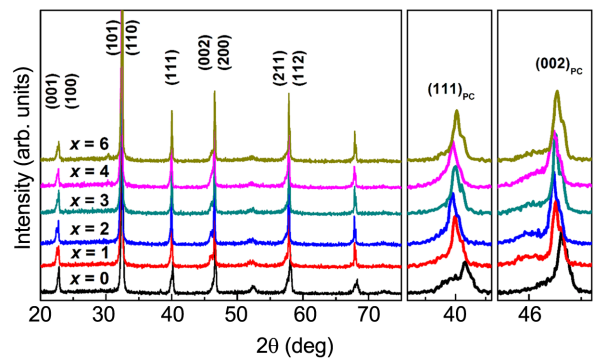


**Fig. 2.** X-ray diffraction patterns of BNBT $x$ Nb ceramics.

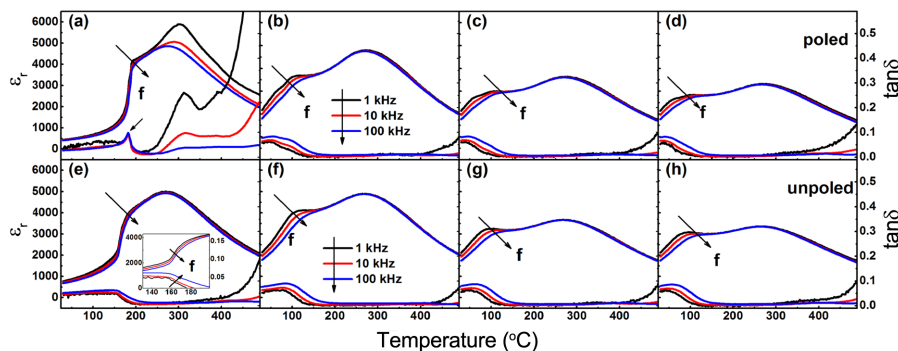


**Fig. 3.** Temperature dependence of permittivity and  $\tan \delta$  of BNBT $x$ Nb ceramics for poled (top) and unpoled (bottom) samples. For (a) and (e),  $x = 0$ ; for (b) and (f),  $x = 2$ ; for (c) and (g),  $x = 4$ ; for (d) and (h),  $x = 6$  at% of Nb-doped BNBT ceramics.

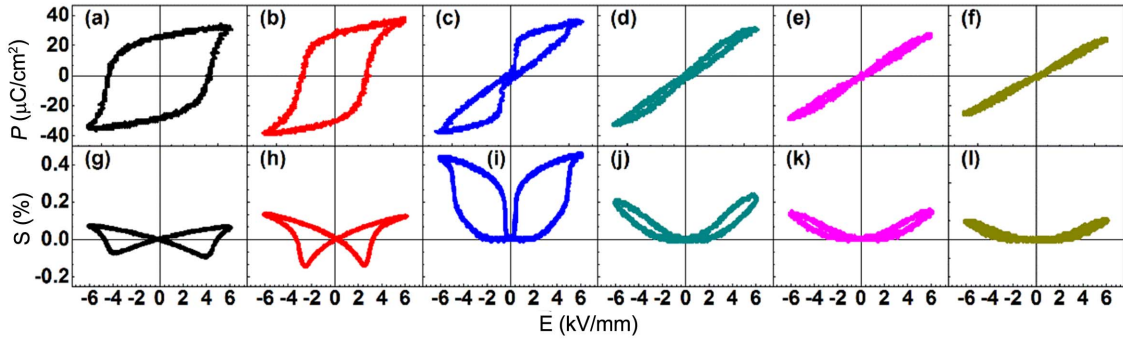


**Fig. 4.** Polarization (top) and strain (bottom) hysteresis of Nb-doped BNBT ceramics. (a) and (g),  $x = 0$ ; (b) and (h),  $x = 1$ ; (c) and (i),  $x = 2$ ; (d) and (j),  $x = 3$ ; (e) and (k),  $x = 4$ ; and (f) and (l),  $x = 6$  at% Nb-doped BNBT ceramics.

In the case of relaxor ferroelectrics, an additional dielectric anomaly is expected to appear when the materials are electrically poled below their freezing temperature.<sup>18)</sup> This additional feature can be easily seen in BNBT0Nb as a frequency independent discontinuity in  $\tan \delta$  (the arrow in Fig. 3(a)). This is commonly referred to as a ferroelectric-to-relaxor phase transition, in which a field-induced FE state with a long range order converts back to an ergodic relaxor (ER) state; the temperature for this change is denoted as  $T_{F-R}$ .<sup>19)</sup>

The value of  $T_{F-R}$  and the dielectric maximum temperature ( $T_m$ ) for the BNBT0Nb ceramics are around 180 °C and 300 °C, respectively. However, no discerned  $T_{F-R}$  can be observed when the concentration level of Nb exceeds 1 at%, which implies that the  $T_{F-R}$  of these compositions lies below room temperature. The downward shift of  $T_{F-R}$  suggests a compositionally-induced ferroelectric-to-relaxor phase transition<sup>19,20)</sup> due to the presence of Nb. However, it is interesting to note that electrical poling still has an influence on the values of  $\epsilon_r$  and  $\tan \delta$  for BNBT2Nb, BNBT4Nb, and even BNBT6Nb at around 100 °C, implying that the nonergodicity of BNBTxNb may not be completely removed within the currently applied doping level.<sup>21)</sup>

Figure 4 presents the polarization ( $P-E$ ) and strain ( $S-E$ ) hysteresis curves of BNBTxNb ceramics. Typical ferroelectric hysteresis curves, represented by square-type polarization and butterfly-shaped strain hysteresis, were observed for BNBT0Nb and BNBT1Nb ceramics, which have large remanent polarizations  $P_r$  of 25 and 26  $\mu\text{C}/\text{cm}^2$  and coercive fields  $E_c$  of 4.4 and 2.8 kV/mm. However, one of the most interesting features is the comparable maximum polarization ( $P_{\text{max}}$ ) values regardless of the compositions, while a drastic change in  $P_r$  is evident, especially when  $x = 2$ .

On the other hand, the change in the strain behavior is rather complicated. At  $x = 1$ , both the negative strain ( $S_{\text{neg}}$ ) and the maximum strain ( $S_{\text{max}}$ ) are enhanced, indicating that the material becomes softened due to easier domain wall motions.<sup>19)</sup> However, a further increase in Nb concentration seems to result in an increase in  $S_{\text{max}}$ , though  $S_{\text{neg}}$  is completely annihilated. Especially, when  $x = 2$ , this unusual change leads to a unipolar strain  $S_{\text{uni}}$  of 0.46 %, which corresponds to the large-stroke actuator's figure of

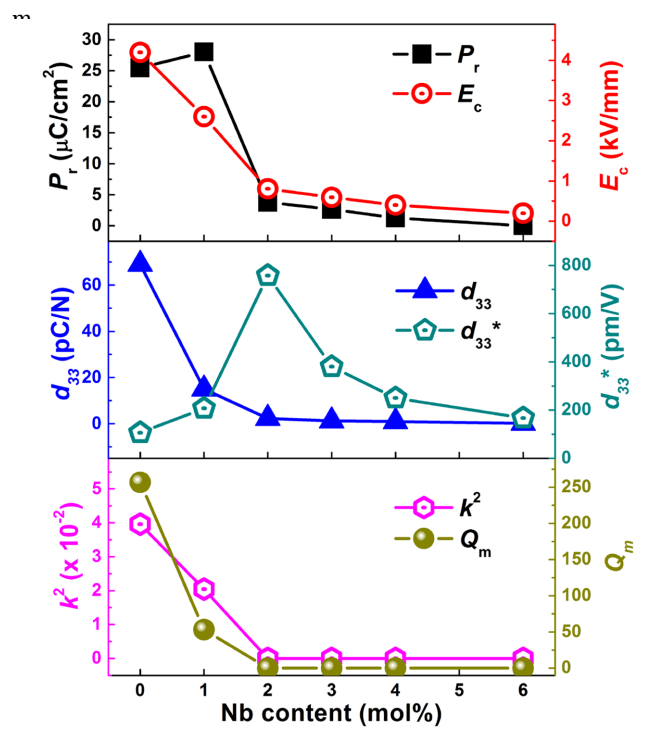


**Fig. 5.** Variation of  $P_r$ ,  $E_c$ ,  $d_{33}$ ,  $d_{33}^*$ ,  $k^2$ , and  $Q_m$  of BNBTxNb ceramics.

merit  $S_{\text{max}}/E_{\text{max}}$  of 767 pm/V.

Figure 5 provides a summary of the values of  $P_r$ ,  $E_c$ , the normalized  $d_{33}^*$  (i.e.,  $S_{\text{max}}/E_{\text{max}}$ ), the Berlincourt piezoelectric constant ( $d_{33}$ ), planar piezoelectric coupling coefficient ( $k^2$ ), and the electromechanical quality factor ( $Q_m$ ) as a function of Nb content. The values of  $P_r$ ,  $E_c$ ,  $d_{33}^*$ ,  $d_{33}$ ,  $k^2$ , and  $Q_m$  for BNBT0Nb ceramics were 25  $\mu\text{C}/\text{cm}^2$ , 4.4 kV/mm, 106 pm/V, 69 pC/N, 21%, and 250, respectively.

All the parameters similarly decrease with increasing Nb content, except for  $d_{33}^*$ . This trend suggests that the stability of long-range ferroelectric order in BNBT ceramics introduced by the application of an electric field is weakened by the presence of Nb as a donor dopant. At the

moment, the exact mechanism for how the introduced donor element destabilizes the ferroelectric long-range order is unclear. However, given that the origin of relaxor behaviors is closely related to the degree of random fields,<sup>22)</sup> the charge balance mechanism when BNBT accommodates the donor dopants is highly likely the formation of relatively immobile defect dipoles with A-site cation vacancies rather than electronic compensation.<sup>23-26)</sup>

#### 4. Conclusions

Lead-free Nb-doped BNBT ceramics have been synthesized using conventional solid state reaction method. Nb doping was found to induce a downward shift of  $T_{F-R}$ , suggesting a compositionally-induced ferroelectric-to-relaxor phase transition. Consequently,  $d_{33}^*$  was drastically enhanced, while  $P_r$ ,  $E_c$ ,  $d_{33}$ ,  $k^2$ , and  $Q_m$  were simultaneously degraded with increasing Nb concentration. The highest value of  $d_{33}^*$  was  $\approx 767$  pm/V, which corresponds to  $S_{uni}$  of 0.46 % at  $x = 2$ .

#### Acknowledgments

This work was supported by the National Research Foundation of Korea (NRF) Grant (2012K1A2B1A03000668). JSL would like to credit the financial support by the National Research Foundation of Korea (NRF) Grant (2013R1A1A2058917). YMK acknowledges the financial support from the National Research Foundation of Korea (NRF) Grant (2013R1A1A2063219).

#### REFERENCES

1. J. Rödel, W. Jo, K. T. P. Seifert, E.-M. Anton, T. Granzow, and D. Damjanovic, "Perspective on the Development of Lead-Free Piezoceramics," *J. Am. Ceram. Soc.*, **92** [6] 1153-77 (2009).
2. J. Rödel, K. G. Webber, R. Dittmer, W. Jo, M. Kimura, and D. Damjanovic, "Transferring Lead-Free Piezoelectric Ceramics into Application," *J. Eur. Ceram. Soc.*, **35** [6] 1659-81 (2015).
3. W. Jo, R. Dittmer, M. Acosta, J. Zang, C. Groh, E. Sapper, K. Wang, and J. Rödel, "Giant Electric-Field-Induced Strains in Lead-Free Ceramics for Actuator Applications-Status and Perspective," *J. Electroceram.*, **29** [1] 71-93 (2012).
4. C.-H. Hong, H.-P. Kim, B.-Y. Choi, H.-S. Han, J. S. Son, C.-W. Ahn, and W. Jo, "Lead-Free Piezoceramics-Where to Move on?," *J. Materiomics*, **2** [1] 1-24 (2016).
5. T. Takenaka, K.-I. Maruyama, and K. Sakata, "(Bi<sub>1/2</sub>Na<sub>1/2</sub>)TiO<sub>3</sub>-BaTiO<sub>3</sub> System for Lead-Free Piezoelectric Ceramics," *Jpn. J. Appl. Phys.*, **30** [9S] 2236-39 (1991).
6. A. Sasaki, T. Chiba, Y. Mamiya, and E. Otsuki, "Dielectric and Piezoelectric Properties of (Bi<sub>0.5</sub>Na<sub>0.5</sub>)TiO<sub>3</sub>-(Bi<sub>0.5</sub>K<sub>0.5</sub>)TiO<sub>3</sub> Systems," *Jpn. J. Appl. Phys.*, **38** [9S] 5564-67 (1999).
7. S.-T. Zhang, A. B. Kouniga, E. Aulbach, H. Ehrenberg, and J. Rödel, "Giant Strain in Lead-Free Piezoceramics Bi<sub>0.5</sub>Na<sub>0.5</sub>TiO<sub>3</sub>-BaTiO<sub>3</sub>-K<sub>0.5</sub>Na<sub>0.5</sub>NbO<sub>3</sub> System," *Appl. Phys. Lett.*, **91** [11] 112906 (2007).
8. K.-N. Pham, A. Hussain, C.-W. Ahn, W. Kim, S. J. Jeong, and J.-S. Lee, "Giant Strain in Nb-Doped Bi<sub>0.5</sub>(Na<sub>0.82</sub>K<sub>0.18</sub>)<sub>0.5</sub>TiO<sub>3</sub> Lead-Free Electromechanical Ceramics," *Mater. Lett.*, **64** [20] 2219-22 (2010).
9. K.-N. Pham, H. B. Lee, H.-S. Han, J.-K. Kang, J.-S. Lee, A. Ullah, C.-W. Ahn, and I. W. Kim, "Dielectric, Ferroelectric, and Piezoelectric Properties of Nb-Substituted Bi<sub>1/2</sub>(Na<sub>0.82</sub>K<sub>0.18</sub>)<sub>1/2</sub>TiO<sub>3</sub> Lead-Free Ceramics," *J. Kor. Phys. Soc.*, **60** [2] 207-11 (2012).
10. A. Ullah, R. A. Malik, A. Ullah, D. S. Lee, S. J. Jeong, J.-S. Lee, I. W. Kim, and C.-W. Ahn, "Electric-Field-Induced Phase Transition and Large Strain in Lead-Free Nb-Doped BNKT-BST Ceramics," *J. Eur. Ceram. Soc.*, **34** [1] 29-35 (2014).
11. R. A. Malik, J.-K. Kang, A. Hussain, C.-W. Ahn, H.-S. Han, and J.-S. Lee, "High Strain in Lead-Free Nb-Doped Bi<sub>1/2</sub>(Na<sub>0.84</sub>K<sub>0.16</sub>)<sub>1/2</sub>TiO<sub>3</sub>-SrTiO<sub>3</sub> Incipient Piezoelectric Ceramics," *Appl. Phys. Express*, **7** [6] 061502 (2014).
12. K. T. Lee, J. S. Park, J. H. Cho, Y. H. Jeong, J. H. Paik, and J. S. Yun, "The Study on the Phase Transition and Piezoelectric Properties of Bi<sub>0.5</sub>(Na<sub>0.78</sub>K<sub>0.22</sub>)<sub>0.5</sub>TiO<sub>3</sub>-LaMnO<sub>3</sub> Lead-free Piezoelectric Ceramics," *J. Korean Ceram. Soc.*, **52** [4] 237-42 (2015).
13. W. Jo, T. Granzow, E. Aulbach, J. Rödel, and D. Damjanovic, "Origin of the Large Strain Response in (K<sub>0.5</sub>Na<sub>0.5</sub>)NbO<sub>3</sub>-Modified (Bi<sub>0.5</sub>Na<sub>0.5</sub>)TiO<sub>3</sub>-BaTiO<sub>3</sub> Lead-Free Piezoceramics," *J. Appl. Phys.*, **105** [9] 094102 (2009).
14. W. Jo, S. Schaab, E. Sapper, L. A. Schmitt, H.-J. Kleebe, A. J. Bell, and J. Rödel, "On the Phase Identity and Its Thermal Evolution of Lead Free (Bi<sub>1/2</sub>Na<sub>1/2</sub>)TiO<sub>3</sub>-6mol% BaTiO<sub>3</sub>," *J. Appl. Phys.*, **110** [7] 074106 (2011).
15. A. Glazounov, A. Tagantsev, and A. J. Bell, "Evidence for Domain-Type Dynamics in the Ergodic Phase of the PbMg<sub>1/3</sub>Nb<sub>2/3</sub>O<sub>3</sub> Relaxor Ferroelectric," *Phys. Rev. B*, **53** [17] 11281-84 (1996).
16. A. J. Bell, "Calculations of Dielectric Properties from the Superparaelectric Model of Relaxors," *J. Phys. Condens. Matter*, **5** [46], 8773 (1993).
17. W. Jo, J.-B. Ollagnier, J.-L. Park, E.-M. Anton, O. J. Kwon, C. Park, H.-H. Seo, J.-S. Lee, E. Erdem, R.-A. Eichel, and J. Rödel, "CuO as a Sintering Additive for (Bi<sub>1/2</sub>Na<sub>1/2</sub>)TiO<sub>3</sub>-BaTiO<sub>3</sub>-(K<sub>0.5</sub>Na<sub>0.5</sub>)NbO<sub>3</sub> Lead-Free Piezoceramics," *J. Eur. Ceram. Soc.*, **31** [12] 2107-17 (2011).
18. D. Viehland, S. J. Jang, L. E. Cross, and M. Wuttig, "Freezing of the Polarization Fluctuations in Lead Magnesium Niobate," *J. Appl. Phys.*, **68** 2916-21 (1990).
19. K. Wang, A. Hussain, W. Jo, and J. Rödel, "Temperature-Dependent Properties of (Bi<sub>1/2</sub>Na<sub>1/2</sub>)TiO<sub>3</sub>-(Bi<sub>1/2</sub>K<sub>1/2</sub>)TiO<sub>3</sub>-SrTiO<sub>3</sub> Lead-Free Piezoceramics," *J. Am. Ceram. Soc.*, **95** [7] 2241-47 (2012).
20. H.-S. Han, W. Jo, J.-K. Kang, C.-W. Ahn, I. W. Kim, K.-K. Ahn, and J.-S. Lee, "Incipient Piezoelectrics and Electrostriction Behavior in Sn-Doped Bi<sub>1/2</sub>(Na<sub>0.82</sub>K<sub>0.18</sub>)<sub>1/2</sub>TiO<sub>3</sub> Lead-Free Ceramics," *J. Appl. Phys.*, **113** [15] 154102 (2013).
21. H.-S. Han, W. Jo, J. Rödel, I.-K. Hong, W. P. Tai, and J.-S. Lee, "Coexistence of Ergodicity and Nonergodicity in

- LaFeO<sub>3</sub>-Modified Bi<sub>1/2</sub>(Na<sub>0.78</sub>K<sub>0.22</sub>)<sub>1/2</sub>TiO<sub>3</sub> Relaxors,” *J. Phys. Condens. Matter.*, **24** [36] 365901 (2012).
22. V. Westphal, W. Kleemann, and M. Glinchuk, “Diffuse Phase Transitions and Random-Field-Induced Domain States of the “Relaxor” Ferroelectric Pb(Mg<sub>1/3</sub>Nb<sub>2/3</sub>)O<sub>3</sub>,” *Phys. Rev. Lett.*, **68** [6] 847-50 (1992).
23. F. D. Morrison, D. C. Sinclair, and A. R. West, “Electrical and Structural Characteristics of Lanthanum-Doped Barium Titanate Ceramics,” *J. Appl. Phys.*, **86** [11] 6355-66 (1999).
24. F. D. Morrison, D. C. Sinclair, and A. R. West, “An Alternative Explanation for the Origin of the Resistivity Anomaly in La-Doped BaTiO<sub>3</sub>,” *J. Am. Ceram. Soc.*, **84** [2] 474-76 (2001).
25. F. D. Morrison, D. C. Sinclair, and A. R. West, “Doping Mechanisms and Electrical Properties of La-Doped BaTiO<sub>3</sub> Ceramics,” *Int. J. Inorg. Mater.*, **3** [8], 1205-10 (2001).
26. C. L. Freeman, J. A. Dawson, H.-R. Chen, L. Ben, J. H. Harding, F. D. Morrison, D. C. Sinclair, and A. R. West, “Energetics of Donor-Doping, Metal Vacancies, and Oxygen-Loss in A-Site Rare-Earth-Doped BaTiO<sub>3</sub>,” *Adv. Func. Mater.*, **23** [31] 3925-28 (2013).